Journal of Materials Chemistry A

Synergistic Catalysis of Au–Cu/TiO2-NB Nanopaper in Aerobic Oxidation of Benzyl Alcohol

Journal:	*Journal of Materials Chemistry A*
Manuscript ID:	TA-ART-03-2014-001503.R1
Article Type:	Paper
Date Submitted by the Author:	09-Jul-2014

Complete List of Authors:	Jia, Qinqin; Shandong university, School of Chemistry and Chemical Engineering Zhao, Dongfang; Shandong university, State Key Laboratory of Crystal Materials Tang, Bin; Shandong university, School of Chemistry and Chemical Engineering Zhao, Na; Shandong university, School of Chemistry and Chemical Engineering Li, Haidong; Shandong University, State Key Laboratory of Crystal Materials Sang, Yuanhua; Shandong university, State Key Laboratory of Crystal Materials Bao, Nan; Shandong university, School of Environmental Science and Engineering Zhang, Xiaomei; Shandong university, School of Chemistry and Chemical Engineering xu, xiaohong; Shandong University, School of Chemistry and Chemical Engineering Liu, Hong; Shandong university, State Key Laboratory of Crystal Materials

Cite this: DOI: 10.1039/c0xx00000x

www.rsc.org/xxxxxx

ARTICLE TYPE

Synergistic Catalysis of Au–Cu/TiO_2-NB Nanopaper in Aerobic Oxidation of Benzyl Alcohol

Qinqin Jia[a], Dongfang Zhao[b], Bin Tang[a], Na Zhao[a], Haidong Li[b], Yuanhua Sang[b], Nan Bao[c], Xiaomei Zhang[a], Xiaohong Xu*[a] and Hong Liu*[b]

Received (in XXX, XXX) Xth XXXXXXXXX 20XX, Accepted Xth XXXXXXXXX 20XX
DOI: 10.1039/b000000x

Au-Cu bimetallic nanoparticles supported on TiO_2-nanobelt (TiO_2-NB) have been designed and synthesized by one pot photodeposition-galvanic replacement method. The TEM observation revealed that small-sized metal nanoparticles (less than 2 nm) uniformly and finely dispersed on TiO_2 nanobelt. Characterization by XRD coupled with XPS demonstrated that the Au-Cu bimetallic nanoparticles are composed with an Au-rich core/CuO_x shell structure. The as-synthesized one dimensional Au-Cu/TiO_2-NB nanostructure can be easily assembled into paper-like porous monolithic catalyst and applied in the heterogeneous catalysis. The formed bimetallic nanopaper catalyst presented synergistically enhanced activity and improved stability for catalyzing the aerobic oxidation of benzyl alcohol compared to their monometallic counterparts. It is likely that the Au-CuO_x heterostructure is responsible for the superior catalytic properties of the bimetallic Au-Cu/TiO_2-NB catalysts, and the catalytic activity can be significantly affected by the Au/Cu ratio. The uniform and high dispersion of metal nanoparticles on TiO_2 nanobelts are also believed to contribute to the stability of Au–Cu/TiO_2-NB catalysts, suggesting that the one-dimensional TiO_2 nanobelts are desirable support for the preparation of nanoscale metal catalysts.

1. Introduction

It is well established that the catalytic properties of bimetallic nanoparticles are superior to their monometallic counterparts because of their tunable and synergistic effect.[1-3] Many researchers have made great efforts to develop various nanostructured bimetallic catalysts via different synthesis approaches. In particular, the synthesis and synergistic catalysis of Au-based bimetallic nanocatalysts have received considerable interest along with the "gold rush" in catalysis.[1-5] Exemplarily, various Au-Cu bimetallic structures have recently been constructed and applied in many important chemical reactions, such as low temperature CO oxidation,[6-9] the preferential oxidation of CO in H_2-rich gas,[10] propane epoxidation,[11-13] aerobic oxidation of alcohols and other organic matters.[14-17] Most of them showed enhanced activity and improved stability compared to monometallic counterparts.[6-9, 13-17]

As it is known, the catalytic properties of Au-based nanocatalysts strongly depend on their composition,[1-5] size and interaction with the support.[18-22] Higher catalytic activity is generally expected for smaller particles due to the large quantity of high active sites with the increased specific surface area. However, extremely small size tends to cause deactivation due to the occurrence of particle sintering during the catalytic process at elevated temperature. Bimetallic structure comprising Au with non-noble metal (such as Cu) can mitigate the particle sintering on account of the phase segregation upon treatment in an oxidizing atmosphere or under catalytic reaction condition, i.e. Cu oxides are easily formed and enriched on the particle surface. The oxides will decorated on Au-rich core in the forms of patches or shells and formed an Au-CuO_x heterostructure.[5] The formed oxides or Au-oxide interfaces were supposed to be the active sites for the activation of oxygen molecules and account for the enhanced activity of bimetallic systems for the aerobic oxidation reactions.[8,10,17] Meanwhile, these oxides can act as a shield to suppress the particle growth during reaction and therefore endow an improved stability.[5,23] Furthermore, for the application of heterogeneous catalysis, metal nanoparticles or clusters normally need to be finely dispersed on oxide supports to achieve high mass activity and resistance to aggregation. For these supported

catalysts, the collective properties such as the relative spatial distribution of nanoparticles and particle size distribution were found to have pronounced impact on catalyst stability.[24,25] Generally, high dispersed nanoparticles with equal sizes (minimum driving force for ripening) and broad neighbour-distance distributions are ideal for a growth-resistant catalyst. However, it is quite common for many technical catalysts in which the spatial distributions of metal nanoparticles on supports are non-uniform, which has significant effect on metal particle growth.

Titanium dioxide (TiO_2) is a well-known support material for noble metallic catalysts because of its low cost, chemical stability, and environment-friendly properties. One-dimensional nanomaterials (e.g. TiO_2 nanobelts), which have comparable large surface area to the nanoparticles, peculiar formability and integratability, can function as support materials for anchoring catalytically active metal species. Generally, the well-crystallized TiO_2 nanobelts with clean and smooth surface can be synthesized by the controllable hydrothermal method easily.[26-29] In our previous work,[30] well-dispersed small Au-Ag bimetallic nanoparticles deposited on TiO_2 nanobelts have been prepared. Most significantly, these formed nanostructures can be readily assembled into paper-like porous monolithic catalyst which exhibited high activity and stability for the selective oxidation of benzyl alcohol to benzaldehyde at elevated temperature. In comparison with the common supported nanocatalysts based on silica gel or other porous supports, the as-prepared nanopaper catalysts not only have highly porous structure to ensure the accessibility of active sites, but also enable the even dispersion of metal nanoparticles within the three-dimensional spatial framework. All these properties mentioned above endow the catalysts with excellent catalytic activity and stability.

As is well known, TiO_2 is an excellent photocatalyst and has attracted great attention for its promising applications in photocatalysis and photovoltaics.[31-34] For the preparation of TiO_2 supported catalysts, the photodeposition has been shown to be a simple "green" approach for obtaining clean metallic metal oxide nanoparticles highly dispersed on TiO_2 surface.[35,36] In previous work, we have developed a facile successive photodeposition-galvanic replacement approach to synthesize Au-Ag/TiO_2-NB nanostructure.[30] However, the low electronegativity of 1.9 for metallic Cu leads to nanoparticulate Cu can be immediately oxidized when they are exposed in air, and there are only few reports about metallic Cu nanoparticles photodeposited on TiO_2 or other semiconductor photocatalysts.[37] Hence, it is difficult to synthetize Au-Cu/TiO_2-NB nanostructure via the successive photodeposition-galvanic replacement approach.

In the present study, we report the fabrication of Au-Cu/TiO_2-NB nanostructure for the first time by one-pot photodeposition-galvanic replacement method. The synthesis strategy is depicted in Scheme 1. During the preparation process, we managed to control the metal nanoparticle sizes by regulating the photodeposition time, and adjust the Au-Cu composition via tuning the ratio of Cu^{2+} and $AuCl_4^-$ in the mixed solution. Based on these Au-Cu/TiO_2-NB nanostructures, a monolithic paper-structured catalyst was fabricated using the modified paper-making process which was depicted in our earlier work.[30] The aerobic oxidation of benzyl alcohol was used as a probe reaction to evaluate the catalytic properties of as-synthesized Au-Cu/TiO_2-NB nanopaper catalysts.

2. Experimental

2.1 Materials

Titania (P25, Evonik, 50m^2g^{-1}, 80% Anatase, 20% Rutile) powder was hydrothermally treated in concentrated NaOH aqueous solution to synthesize the TiO_2 nanobelts.[30,38-39] Acros Chemicals ($HAuCl_4$) was used as a gold precursor and copper acetate (Cu$(CH_3COO)_2$) as a copper precursor, directly used without further treatment. Sodium hydroxide (NaOH) and ethyl alcohol (CH_3CH_2OH) were all of analytical reagent grade. Ultrapure water was used all through our experiments.

2.2 Synthesis of M/TiO_2-NB nanostructure (M=Au, Cu, Au-Cu)

Synthesis of Au-Cu/TiO_2-NB nanostructure. The Au-Cu/TiO_2-NB nanostructures were prepared by a one-pot photocatalytic-galvanic replacement approach. Firstly, 0.1g TiO_2 nanobelts were dispersed evenly in 2 mL 0.1 M Cu $(CH_3COO)_2$ aqueous solution and 20 mL CH_3CH_2OH. The turbid liquid was deaerated by N_2 gas flow for 30 min, and adjusted the pH of the precursor solution to 7 with NaOH aqueous solution. Secondly, the obtained solution was irradiated for 20 min under a 500W Xe lamp to photodeposit Cu nanoparticles onto TiO_2 nanobelts. Then, 15 mL $HAuCl_4$ (0.003 M) aqueous solution deaerated by N_2 gas flow was added into the irradiated solution to perform the galvanic replacement reaction between photodeposited Cu particles and

$AuCl_4^-$ for 15 min in dark. Vigorous magnetic stirring and nitrogen purge to eliminate oxygen were maintained during entire process. The resulting product was filtrated and washed with ultrapure water for several times, and dried in vacuum stove for 24 h.

Synthesis of Cu/TiO_2-NB nanostructure. The Cu/TiO_2-NB was synthesized by the same photodeposition method as that for Au-Cu/TiO_2-NB without the galvanic replacement process.

Synthesis of Au/TiO_2-NB nanostructure. The Au/TiO_2-NB was prepared via the photodeposition method. 0.1 g TiO_2 nanobelts and 1 mL 0.5 M $HAuCl_4$ were added into the mixture of 0.02 M sodium citrate and 0.1 M NaOH solution. The mixed solution was irradiated by the Xe lamp for 2 minutes under vigorous magnetic stirring. The resulting product was filtrated and washed with ultrapure water for several times, and dried in vacuum stove for 24 h.

2.3 Characterization

X-ray diffraction (XRD) analysis was conducted on a German Bruker D8 X-ray diffractometer. Transmission electron microscopy (TEM) and high resolution transmission electron microscopy (HRTEM) images were obtained with a JOEL JEM 2100 microscope. HITACHI S-4800 field emission scanning electron microscope (FE-SEM) was used to characterize the morphologies. X-ray photoelectron spectroscopy (XPS) data were acquired on a Thermo ESCALAB 210 X-ray photoelectron spectrometer and the binding energies were determined utilizing C1s spectrum as reference at 285.0 eV. The UV-vis absorption spectra were recorded on a Shimadzu U-2400PC spectrophotometer with barium sulfate as a standard for the background correction. The metal loading and the Au/Cu molar ratio in the samples were detected by inductively coupled plasma spectrometer (ICP-AES) on an IRIS Intrepid II XSP instrument (Thermo Electron Corporation).

2.4 Catalytic reaction tests

The gas-phase selective oxidation of benzyl alcohol was carried out with a continuous flow fixed-bed microreactor (8 mm i. d.). In the catalytic test, four pieces Au-Cu/TiO_2-NB paper (8 mm in diameter and total weight of 20 mg) were stacked vertically on a Teflon ring fixed to the inner wall of the reactor, and the process was carried out at atmospheric pressure and a lower reaction temperature of 240°C. The gas streams (44 mL/min, O_2/N_2=21:79) were supplied by mass flow controllers, and benzyl alcohol (20 μL/min, WHSV of 63 h^{-1}) was fed continuously through a syringe pump. Liquid vaporization occurred in the preheater prior to the catalytic reaction bed. The condensable reaction products and the unreacted benzyl alcohol were cooled and collected using a cold trap (0 °C). Then, the mixture was analyzed with a Shimadzu Type GC-14C equipped with a flame ionization detector, using a SGE-30QC2/AC5 capillary column and N_2 as carrier gas. 1-Butanol was employed as an internal standard. GC-MS (Thermo Trace GC Ultra DSQ) was also employed to determine the reaction products.

3. Results and Discussion

Bimetallic Au-Cu/TiO_2-NB nanostructures were prepared by one-pot photodeposition-galvanic replacement method. Inductively coupled plasma (ICP) analysis indicated that the metal loading and Au/Cu ratio in Au-Cu/TiO_2-NB nanostructures are tuneable by simply controlling the composition of precursor solution, photodeposition time and galvanic replacement time. Herein, we regulate the Cu loading by varying the photodeposition time, keeping the Au loading at about 2 wt. %. No diffraction peaks of Au or Cu species were found in the XRD pattern of the as-prepared Au-Cu/TiO_2-NB sample (Fig. S1, ESI†), which may be due to the rather low loading and small sizes of metal nanoparticles. In order to characterize the Au-Cu bimetallic structure, XRD pattern of Au-Cu/TiO_2-NB sample with several times of metal loading amount was acquired (Fig. S2, ESI†), As can be seen, the strong diffraction peaks are indexed to the TiO_2 nanobelts support, the small diffraction peaks at 2θ=38.2, 44.3 and 64.5 can be attributed to the face-centered cubic (fcc) structure of metallic Au (PDF No. 01-1172). Diffraction peaks at 2θ=36.5 and 42.4 are likely to be Cu^+, and the other peaks at 2θ=35.4 and 38.8 are mostly to be Cu^{2+}. However, no characteristic peaks related to metallic Cu^0 are observed in the XRD pattern. It is obvious that Cu was successfully loaded on TiO_2 nanobelts via photodeposition, and the following galvanic replacement process produced the Au-Cu bimetallic nanostructure using the photodeposited Cu particles as templates. Evidently, due to the Cu nanostructures are easily oxidized under ambient or aqueous conditions,[40,41] the phase segregation occurred in the freshly-formed Au-Cu/TiO_2-NB nanostructure when exposed to air during sample handling, and thus the element Cu in Au-Cu/TiO_2-NB is detected to be mainly in the form of copper oxide species (CuO_x). These Cu oxides would

enrich on the surface and resulted in an Au-rich core and CuO_x shell in the nanoparticles, so the as-prepared Au-Cu/TiO_2-NB samples can be regarded as Au-CuO_x/TiO_2-NB nanostructures.

Fig. 1a, b present the TEM images of photodeposited Au and Cu nanoparticles on TiO_2 nanobelt as well as the as-prepared Au-Cu/TiO_2-NB nanostructure. For both Au/TiO_2-NB and Cu/TiO_2-NB nanostructures, it can be seen that large amounts of small-sized metal nanoparticles are dispersed uniformly over TiO_2 nanobelt which has a width of 50-200 nm and length of up to dozens of micrometers. The corresponding histograms of particle size distribution for Au and Cu show an average size of 1.7 ± 0.1 nm and 2.2 ± 0.1 nm, respectively. The TEM image in Fig. 1c reveals that the obtained Au-Cu/TiO_2-NB nanostructures have similar morphology of small well-dispersed particles on nanobelt compared to that of Cu/TiO_2-NB samples. This feature is just like that observed for the previously synthesized Au-Ag/TiO_2-NB catalyst,[30] demonstrating that the one-dimensional TiO_2 nanobelts are ideal for the preparation of finely dispersed nano-scale metal catalysts. Compared with the porous or particle supports, the clean and flat surface of TiO_2-NB contains less step and kink sites, which might account for the highly and uniformly dispersion of metal clusters or nanoparticles in metal nanopartcles/TiO_2-NB nanostructures. A narrow size distribution with an average diameter of 1.7 ± 0.1 nm (Fig. 1f) was observed, suggesting that the metal particles strongly combine with the TiO_2 nanobelts without leaching or agglomeration during the galvanic replacement process. For comparison, the reaction of pure TiO_2 nanobelts with $HAuCl_4$ solution was carried out under the same conditions, and no formation of Au nanoparticles was detected by TEM.

Fig. 2a and 2b present the HRTEM images of Au-Cu/TiO_2-NB nanostructure. It shows uniform lattice fringes continuously spaced across the surface of TiO_2 nanobelts in the length direction, indicating its single crystalline structured nature. The interplanar distance of 3.36 Å (Fig. 2a, inset) corresponds to the (101) crystal plane of anatase TiO_2. The hemispherical particles anchored to TiO_2 nanobelt are featured with a highly crystallized core and a blurring layer. That is consistent with the XRD analysis that the Au-Cu bimetallic nanoparticles are constructed with Au-CuO_x nanostructure. The measured lattice spacing of particle core is 2.32 Å, a value close to Au (reference value of 2.35 Å in PDF No. 01-1172). Thus, the lattice spacing of the core can be assigned to the cubic Au (111) plane, accounting for the Cu existing could lead to a reduction of lattice parameter of Au. The less intense contrast layer is probably a CuO_x film which is around the Au particle to create an Au-rich core and CuO_x shell structure. The nanostructure of Au-Cu bimetallic particles could be simulated in Fig. 2c.

To obtain more information about the structural feature of bimetallic Au-Cu/TiO_2-NB nanostructure, further characterization have been carried out using XPS analysis and UV-vis diffuse reflectance spectra. Fig. 3a, c-d show the XPS spectra of Au 4f and Cu 2p in bimetallic nanoparticles anchored on TiO_2 nanobelts. For the bimetallic Au-Cu/TiO_2-NB sample, the Au 4f and Cu 2p signals were detected simultaneously in the XPS spectrum, further confirming a galvanic replacement reaction did occur between photodeposited Cu particles and $AuCl_4^-$. The identical binding energies values of 83.0 eV (Au $4f_{7/2}$) and 87.3 eV (Au $4f_{5/2}$) in both Au/TiO_2-NB and Au-Cu/TiO_2-NB match with that of the inert nature of metallic gold (Fig. S3, ESI†) . In Fig. 3c and 3d, the Cu $2p_{3/2}$ and $2p_{1/2}$ regions can be deconvolved into different copper species because of Cu nanostructures are easily oxidized to Cu^+ and Cu^{2+} under ambient or aqueous conditions, and the binding energies of Cu $2p_{3/2}$ in Cu, Cu_2O and CuO are 932.2, 932.6, and 933.2 eV respectively.[42] As seen in Fig. 3c, there are two main XPS peaks at 933.4 and 953.2 eV, which can be assigned to CuO_x for two spin orbit components, viz., Cu $2p_{3/2}$ and Cu $2p_{1/2,}$ and the Cu pieces in Au-Cu/TiO_2-NB nanostructures are contributed by Cu^0 (11.1%), Cu^+ (44.4%) and Cu^{2+} (44.5%). This XPS analysis agrees with the bimetallic particles existed in an Au-core/CuO_x shell structure in Au-Cu/TiO_2-NB.

The UV-vis diffuse reflectance spectra shown in Fig. 3b indicate that, in contrast to only UV absorption at wavelengths below 400 nm for TiO_2 nanobelts, distinct visible light absorption appeared for all three types of metal nanoparticle deposited on TiO_2 nanobelts. The wide absorption peak located at 620 nm for the Au/TiO_2-NB sample is attributed to the surface plasma resonance (SPR) of photodeposited Au nanoparticles.[30] In the case of Cu/TiO_2-NB, the visible light absorption resolves into two bands: one is centered at about 450 nm, the other one is a wide absorption band in the visible and near infra-red regions, indicating that there are at least two species in the CuO_x shell.[43,44] For Au-Cu/TiO_2-NB, it shows a superposition absorption peak of Au/TiO_2-NB and Cu/TiO_2-NB nanostructures. The entire absorption enhancement in the visible region compared to that of Au/TiO_2 is clearly caused by the existence of copper species and

the formation of an Au/CuO_x bimetallic structure.[45,46]

The as-synthesized bimetallic Au–Cu/TiO_2-NB nanostructure (without any pretreatment) was applied as a paper-like structured monolithic catalyst in the selective gas-phase oxidation of benzyl alcohol and compared to the monometallic counterparts. The typical SEM image (Fig. 4a) of these nanopaper catalysts presents the nanobelts overlap in a disordered fashion to form an intersecting 3D porous structure. Fig. 3b and Fig. 4b show digital pictures of the integrated paper-like catalysts and the fixed-bed vertical quartz tubular reactor filled with them. In the catalytic test, 20 mg nanopaper catalysts were stacked vertically on a Teflon ring fixed to the inner wall of the reactor, and the process was carried out at atmospheric pressure and reaction temperature of 220°C ~ 240°C. A high space velocity of 1.55×105 h^{-1} was used to eliminate the mass transfer limitation. As shown in Fig. 4c, it is obvious that all of the photodeposited Au and Cu on TiO_2 nanobelt, as well as the as-synthesized Au-Cu/TiO_2-NB, are active for the oxidation of benzyl alcohol to benzaldehyde with high selectivity. The bimetallic catalyst shows remarkably enhanced activity and improved stability for this reaction compared to monometallic Au and Cu, and a benzyl alcohol conversion of above 50% was obtained at a low temperature of 220°C (Fig. S4, ESI†). As demonstrated above, the metal nanoparticles in Au-Cu/TiO_2-NB are composed of Au-CuO_x heterostructure, i.e. CuO_x patches or shell decorated on Au-rich core. Clearly, such enhanced activity can be ascribed to the cooperative effect of Au and CuO_x species.[8,9,17,47] Furthermore, the activity of Au-Cu/TiO_2-NB nanostructures was found to be very dependent on their composition. Fig. 4d compares the catalytic performances of Au-Cu/TiO_2-NB nanopaper catalysts with different Au/Cu ratios. The benzyl alcohol conversion decreased with the increase of Cu content under the same Au loading, the highest activity (conversion of ~93%) was achieved for the Au-rich sample with a high Au/Cu atomic ratio of ~1:2.3. Such activity dependent on the Cu content in Au-Cu/TiO_2-NB catalysts demonstrated that the existence of much more CuO_x will reduce the accessibility of reactive molecules to the Au active sites and thus decrease the catalytic activity. A high TOF number of 5517 h^{-1} was calculated based on the total number of Au atoms for Au-Cu/TiO_2-NB nanopaper catalysts with the best Au/Cu ratio of 1:2.3 (the reaction temperature of 240°C), which is twice times of the value (2160 h^{-1}) obtained on bimetallic Au-Ag/TiO_2-NB nanopaper catalyst with comparable metal nanoparticle sizes.[30] Similar findings that Au–Ag alloy catalysts were less active for the oxidation of alcohols than Au–Cu alloy catalysts with similar particle sizes were reported by Zhang et al.[16] To further investigate how the Au-CuO_x heterostructure affected the catalytic activity, the Au-Cu/TiO_2-NB (Au/Cu ratio of 1:2.3) catalysts were pretreated with CO (21.2 mL/min N_2 +8.8 mL/min CO) at 300°C for 1 h, and the catalytic performance is presented in Fig 4e. The reduced samples which should have some Au-Cu alloy structure exhibited lowered activity compared to the as-prepared one. The result suggests that the oxides or Au-oxide interface may be the active sites for the activation of oxygen molecules and account for the enhanced activity of bimetallic systems. Similar findings were obtained for CO oxidation and the selective oxidation of ethanol over Au-Cu nanocatalysts, where the Au-CuO_x heterostrcture played an important role in the promoted catalytic activity.[8,9,17,47]

As shown in Fig. 5d, the bimetallic catalysts exhibited high stability (>98%) for benzyl alcohol oxidation at elevated temperature of 240°C, and with the best Au/Cu ratio of 1:2.3, a high and stable benzyl alcohol conversion of ~93% was obtained over 30 h time-on-stream performance. Such high catalytic stability of these catalysts implies that the small Au-Cu particles (sub-2 nm) in the Au-Cu/TiO_2-NB have a high resistance to sintering and structural changing during the benzyl alcohol oxidation reaction at 240 °C. The identical Au 4f binding energies as well as only slight change in the composition of Cu pieces with Cu^0 (11.1% to 8.8%), Cu^+ (44.1% to 44.4%) and Cu^{2+} (44.5% to 47.1%) for fresh and used Au-Cu/TiO_2-NB were measured (Fig. 3a, c and d), suggesting that the Au-Cu/TiO_2-NB nanostructure keeps its electronic structure almost unchanged before and after reaction for 30 h. This means that there is no significant change in the structure and size for the used catalysts. Indeed, only less particle aggregation was observed for the Au-Cu/TiO_2-NB sample after reaction at 240 °C for 30 h (Fig. 5b). The average particle size of Au-Cu nanoparticles only increased to 2.0 ± 0.1 nm (Fig.5c) after reaction for 30 h. The encapsulation effect of CuO_x shell in Au-CuO_x/TiO_2-NB nanostructure may be largely responsible for this high-resistant performance. As detected by XRD, HRTEM and XPS characterizations, the as-synthesized bimetallic catalysts in fact are comprised of an Au-rich core/CuO_x shell heterostructure, and that this core/shell structure can still be observed from the HRTEM image of the sample after reaction for 30 h (Fig. S5, ESI†). So the CuO_x shell

can be regarded as the main constituent for contributing to the stability of the Au-CuO_x/TiO_2-NB catalysts. It is common that the surface oxide can serve as a shield against the agglomeration and growth of metal particles.[5,23] Moreover, the narrow size distribution and the even dispersion of metal nanoparticles on TiO_2 nanobelts which seems ideal for sintering-resistant catalysts should also be considered.[21,24,25] Fig. 5e shows the catalytic performance of Au-Cu/TiO_2-NB catalyst with Au/Cu ratio of 1:2.3 which was stored in ambient environment for three months. A relative lower initial conversion of 79% was obtained, then the reaction rate gradually increased which may be ascribed to the release of adsorbed moisture on catalysts and a same conversion of ~93% that obtained for freshly-prepared sample was reached after reaction for 8 h, further demonstrating the high stability of Au-Cu/TiO_2-NB nanopaper catalyst.

In addition to the above-mentioned high catalytic stability of Au-Cu/TiO_2-NB nanostructure, the high sintering-resistance of TiO_2 nanobelts plays a role in stabilizing the porous structure and the active sites for the nanopaper catalysts. The SEM observation (Fig. 5a) depicts that indeed no sintering among nanobelts has occurred after the reaction at 240 °C for 30 h. Furthermore, the nanopaper catalysts are easily recycled by calcination to remove coke, or through the paper-making process to reassemble them into new paper. In this respect, one dimensional metal nanoparticles/TiO_2-NB nanostructures are desirable for application in catalysis by assembling into nanopaper catalysts.

4 Conclusions

In summary, one pot photodeposition-galvanic replacement method has been developed to synthesize highly dispersed small Au-Cu bimetallic nanoparticles (sub-2 nm) on TiO_2 nanobelts. The resulting Au-Cu/TiO_2-NB nanostructures in which the bimetallic nanoparticles are composed of Au-rich core and CuO_x shell can be easily assembled into paper-like porous monolithic catalyst. The Au-Cu/TiO_2-NB nanopaper catalysts based on these nanostructures exhibited superior catalytic performance for benzyl alcohol aerobic oxidation to benzaldehyde compared to their monometallic counterparts. In the bimetallic catalysts, the Au-CuO_x heterostructure likely contributed to enhance the catalytic activity, while the encapsulation effect of Cu oxides on Au core coupled with the even distribution of metal nanaoparticles on TiO_2 nanobelt seem to ensure the catalytic stability by preventing the particles from aggregating and sintering. Furthermore, the one pot photodeposition-galvanic replacement method could enable to tune the catalytic properties via controlling the ratio of Au and Cu. We expect this work could contribute to designing and assembling nanostructured catalysts with high activity and durability.

Inserting Graphics

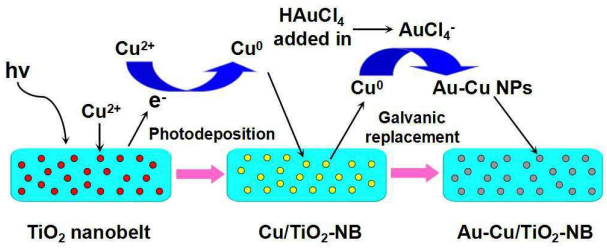

Scheme 1 Schematic illustration for the preparation of Au-Cu/TiO_2-NB

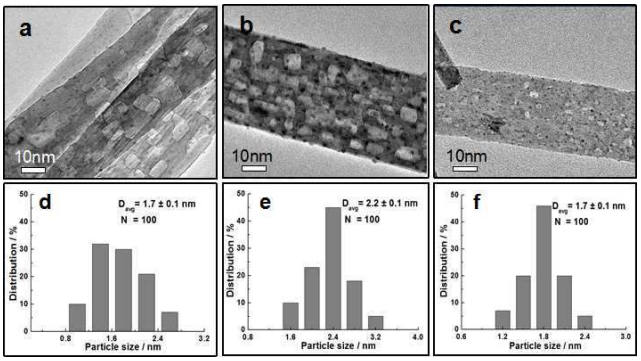

Fig. 1 Representative TEM images of (a) Au/TiO_2-NB, (b) Cu/TiO_2-NB and (c) Au-Cu/TiO_2-NB; the corresponding particle size distribution of (d) Au/TiO_2-NB, (e) Cu/TiO_2-NB and (f) Au-Cu/TiO_2-NB.

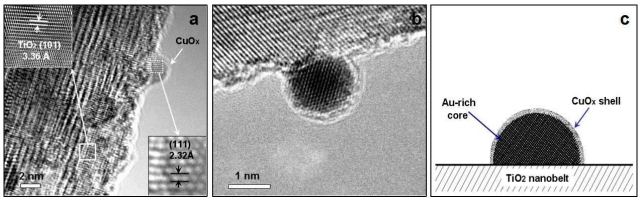

Fig. 2 (a, b) HRTEM images and (c) scheme illustration of Au-Cu/TiO_2-NB nanostructure.

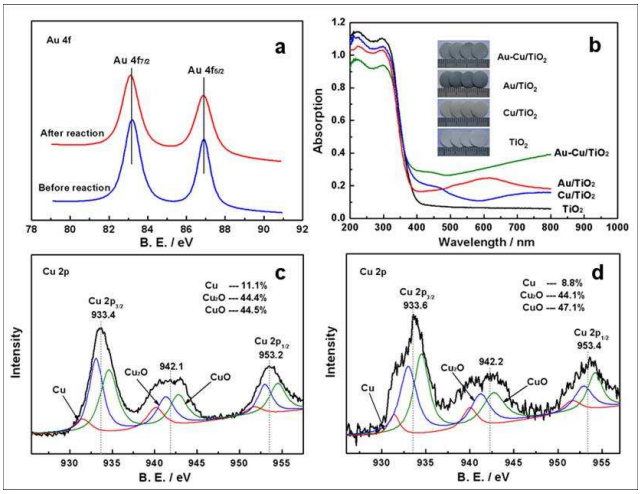

Fig. 3 (a) Au 4f XPS spectra in Au-Cu/TiO_2-NB nanostructure before and after reaction; (b) UV-vis spectra and digital pictures of TiO_2, Au/TiO_2, Cu/TiO_2 and Au-Cu/TiO_2 nanopapers; Cu 2p spectra in Au-Cu/TiO_2-NB nanostructure (c) before and (d) after reaction.

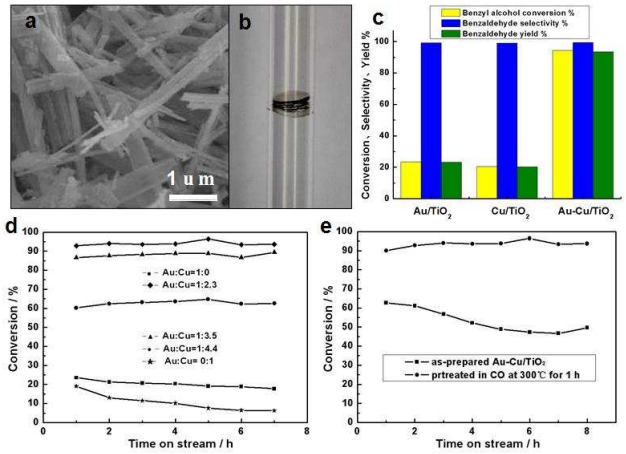

Fig. 4 (a) SEM image and (b) digital picture of nanopaper catalyst bed; (c) the comparison of benzyl alcohol oxidation over Au/TiO_2-NB, Cu/TiO_2-NB and Au-Cu/TiO_2-NB nanopaper catalysts; the catalytic performances of (d) Au-Cu/TiO_2-NB nanopapers with different Au/Cu ratios and (e) Au-Cu/TiO_2-NB as-prepared and pretreated with CO. The reaction temperature is 240°C.

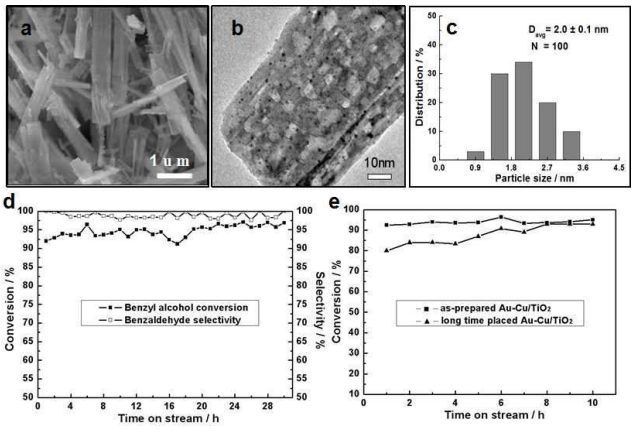

Fig. 5 (a) SEM image, (b) TEM image and (c) the corresponding particle size distribution of Au-Cu/TiO_2-NB after reaction for 30 h at 240 °C; (d) the stability test of Au-Cu/TiO_2-NB nanopaper catalyst for 30 h at 240 °C; (e) time-dependent oxidation of benzyl alcohol over Au-Cu/TiO_2-NB catalyst freshly-prepared and stored for three months.

Acknowledgments

We gratefully acknowledge the financial support of the National Natural Science Foundation of China (Grant No. 51372142, 21176144, 21171106), National Science Fund for Distinguished Young Scholars (NSFDYS: 50925205), Innovation Research Group (IRG: 51321091), the Natural Science Foundation of Shandong Province (ZR2011BM005) and the "100 Talents Program" of Chinese Academy of Sciences.

Notes and references

[a] *Key Laboratory of Colloid and Interface Chemistry, Ministry of Education, School of Chemistry and Chemical Engineering, Shandong University, Jinan 250100, China.*

Email: xhxu@sdu.edu.cn

[b] *State Key Laboratory of Crystal Materials, Shandong University, Jinan, 250100, China.*

E-mail: hongliu@sdu.edu.cn

[c] *School of Environmental Science and Engineering, Shandong University, Jinan 250100, China.*

† Electronic Supplementary Information (ESI) available. See DOI: 10.1039/b000000x/

[1] H. L. Jiang and Q. Xu, *J. Mater. Chem*., 2011, 21, 13705-13725.

[2] D. Wang and Y. Li, *Adv. Mater.*, 2011, 23, 1044-1060.

[3] M. Sankar, N. Dimitratos, P. J. Miedziak, P. P. Wells, C. J. Kiely and G. J. Hutchings, *Chem. Soc. Rev.*, 2012, 41, 8099-8139.

[4] C. L. Bracey, P. R. Ellis and G. J. Hutchings, *Chem. Soc. Rev.*, 2009, 38, 2231-2243.

[5] A. Q. Wang, X. Y. Liu, C. Y. Mou and T. Zhang, *J. Catal.*, 2013, 308, 258-271.

[6] B. L. Zhu, Q. Guo, X. L. Huang, S. R. Wang, S. M. Zhang, S. H. Wu and W. P. Huang, *J. Mol. Catal. A*, 2006, 249, 211-217.

[7] R. J. Chimentão, F. Medina, J. L. G. Fierro, J. Llorca, J. E. Sueiras, Y. Cesteros and P. Salagre, *J. Mol. Catal. A*, 2007, 274, 159-168.

[8] X. Y. Liu, A. Q. Wang, L. Li, T. Zhang, C. Y. Mou and I. F. Lee, *J. Catal.,* 2011, 278, 288-296.

[9] A. Sandoval, C. Louis and R. Zanella, *Appl. Catal., B,* 2013, 140-141, 363-377.

[10] X. Li, S. S. S. Fang, J. Teo, Y. L. Foo, A. Borgna, M. Lin and Z. Zhong, *ACS Catal.*, 2012, 2, 360−369.

[11] J. Llorca, M. Domínguez, C. Ledesma, R. J. Chimentão, F. Medina, J. Sueiras, M. Seco and O. Rossell, *J. Catal.*, 2008, 258, 187-198.

[12] C. L. Bracey, A. F. Carley, J. K. Edwards, P. R. Ellies and G. J. Hutchings, *Catal. Sci. Technol.*, 2011, 1, 76-85.

[13] S. Belin, C. L. Bracey, V. Briois, P. R. Ellis, G. J. Hutching and T. I. Hyde, *Catal. Sci. Technol.*, 2013, 3, 2944-2957.

[14] C. D. Pina, E. Falletta and M. Rossi, *J. Catal.*, 2008, 260, 384-386.

[15] T. Pasini, M. Piccinini, M. Blosi, R. Bonelli, S. Albonetti, G. J. Hutchings and F. Cavani, *Green Chem.*, 2011, 13, 2091-2099.

[16] W. J. Li, A. Q. Wang, X. Y. Liu and T. Zhang, *Appl. Catal., A*, 2012, 433-434, 146-151.

[17] J. C. Bauer, G. M. Veith, L. F. Allard, Y. Oyola, S. H. Overbury and S. Dai, *ACS Catal.*, 2012, 2, 2537-2546.

[18] M. Haruta, *Catal. Today*, 1997, 36, 153-166.

[19] B. K. Min and C. M. Friend, *Chem. Rev.*, 2007, 107, 2709-2724.

[20] J. A. Farmer and C. T. Campbell, *Science*, 2010, 329, 933-936.

[21] J. L. Gong, *Chem. Rev.*, 2012, 112, 2987-3054.

[22] M. C. Daniel and D. Astruc, *Chem. Rev.*, 2004, 104, 293-346.

[23] A. Cao, R. Lu and G. Veser, *Phys. Chem. Chem. Phys.*, 2010, 12, 13499-13510.

[24] G. Prieto, J. Zečević, H. Friedrich, K. P. Jong and P. E. Jongh, *Nat. Mater*., 2013, 12, 34-39.

[25] T. W. Hansen, A. T. DeLaRiva, S. R. Challa and A. K. Datye, *Acc. Chem. Res.,* 2013, 46, 1720-1730.

[26] N. Q. Wu, J. Wang, D. N. Tafen, H. Wang, J. G. Zheng, J. P. Lewis, X. G. Liu, S. S. Leonard and A. Manivannan, *J. Am. Chem. Soc.*, 2010, 132, 6679–6685.

[27] W. J. Zhou, H. Liu, R. I. Boughton, G. J. Du, J. J. Lin, J. Y. Wang and D. Liu, *J. Mater. Chem.*, 2010, 20, 5993–6008.

[28] X. B. Chen and S. S. Mao, *Chem. Rev.*, 2007, 107, 2891-2959.

[29] Z. Y. Yuan and B. L. Su, *Colloids Surf.* , *A*, 2004, 241, 173-183.

[30] Y. Guan, N. Zhao, B. Tang, Q. Q. Jia, X. H. Xu, H. Liu and R. I. Boughton, Chem. Commun., 2013, 49, 11524-11526.

[31] X. Chen, S. S. Mao, *Chem. Rev.*, 2007, 107, 2891-2959.

[32] C.Y. Yang, Z. Wang, T.Q. Lin, X.M. Xie and M.H Jiang, *J. Am. Chem. Soc*, 2013, 135, 17831-17838.

[33] X. B. Chen, L. Liu, P.Y. Yu and S. S. Mao, *Science*, 2011, 331, 746-750.

[34] Z. Wang, C.Y. Yang, T.Q. Lin, X. M. Xie and M. H. Jiang, *Energy Environ. Sci.*, 2013, 6, 3007-3014.

[35] S. C. Chan and M. A. Barteau, *Langmuir*, 2005, 21, 5588-5595.

[36] S. F. Chen, J. P Li, K. Qian, W. P. Xu, Y. Lu, W. X. Huang and S. H. Yu, *Nano Res.*, 2010, 3, 244-255.

[37] E. Kazuma, T. Yamaguchi, N. Sakai and T. Tatsuma, Nanoscale, 2011, 3, 3641-3645.

[38] Y. M. Wang, G. J. Du, H. Liu, D. Liu, S. B. Qin, N. Wang, C. G. Hu, X. T. Tao, J. Jiao, J. Y. Wang and Z. L. Wang, *Adv. Funct. Mater.*, 2008, 18, 1131-1137.

[39] W. J. Zhou, G. J. Du, P. G. Hu, Y. Q. Yin, J. H. Li, J. H. Yu, G. C. Wang, J. X. Wang, H. Liu, J. Y. Wang and H. Zhang. *J. Hazard. Mater.,* 2011, 197, 19-25.

[40] M. S. Jin, G. N. He, H. Zhang, J. Zeng, Z. X. Xie and Y. N. Xia, *Angew. Chem. Int. Ed.*, 2011, 50, 10560-10564.

[41] Z. W. Liu and Y. Bando, *Chem. Phys. Lett.*, 2003, 378, 85-88.

[42] J. F. Moulder, W. F. Stickle, P. E. Sobol and K. E. Bomben, *Physical Electronics*, 1995.

[43] Z. B. Hai, N. E. Kolli, D. B. Uribe, P. Beaunier, M. J. Yacaman, J. Vigneron, A. Etcheberry, S. Sorgues, C. C. Justin, J. Chen and H. Remita, *J. Mater. Chem. A*, 2013, 1, 10829-10835.

[44] S. P. Xu, J. W. Ng, X. W. Zhang, H. W. Bai and D. L. Sun, *Int. J. Hydrogen energ*., 2010, 35, 5254-5261.

[45] S. K. Cushing, J. Li, F. Meng, T. R. Senty, S. Suri, M. Zhi, M. Li, A. D. Bristow and N. Q. Wu, *J. Am. Chem. Soc.*, 2012, 134, 15033-15041.

[46] A. Marimuthu, J. Zhang and S. Linic, *Science*, 2013, 339, 1590-1593.

[47] J. C. Bauer, D. Mullins, M. J. Li, Z. L. Wu, E. A. Payzant, S. H. Overbury and S. Dai, *Phys. Chem. Chem. Phys.*, 2011, 13, 2571-2581.

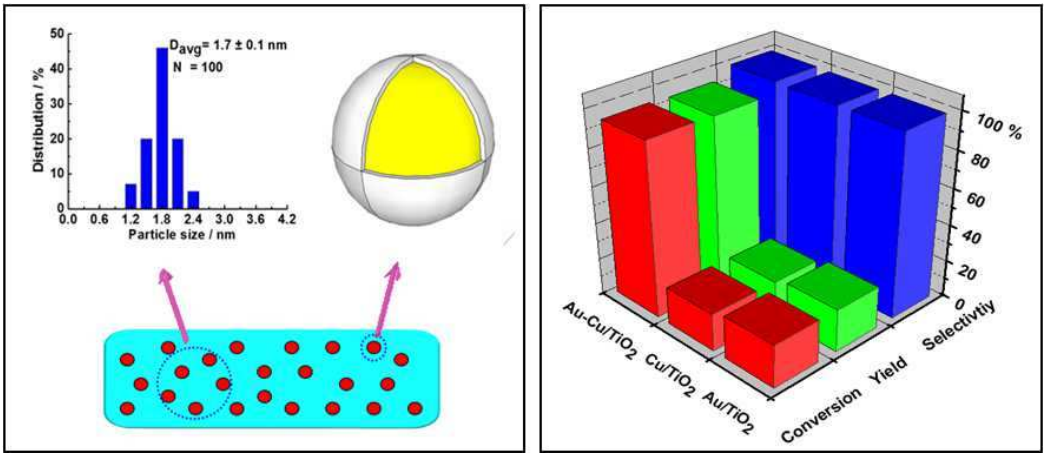

The synergistic catalysis of Au–Cu/TiO_2-NB nanostructure synthesized by one pot photodeposition-galvanic replacement method in benzyl alcohol oxidation